The Experiment Road to the Heavier Quarks and Other Heavy Objects

Jeffrey A. Appel

Fermilab, PO Box 500, Batavia, IL 60510, USA
E-mail: appel@fnal.gov

Abstract. After a brief history of heavy quarks, I will discuss charm, bottom, and top quarks in turn. For each one, I discuss its first observation, and then what we have learned about production, hadronization, and decays - and what these have taught us about the underlying physics. I will also point out remaining open issues. For this series of lectures, the charm quark will be emphasized. It is the first of the heavy quarks, and its study is where many of the techniques and issues first appeared. Only very brief mention is made of CP violation in the bottom-quark system since that topic is the subject of a separate series of lectures by Gabriel Lopez. As the three quarks are reviewed, a pattern of techniques and lessons emerges. These are identified, and then briefly considered in the context of anticipated physics signals of the future; e.g., for Higgs and SUSY particles.

A BRIEF HISTORY OF HEAVY QUARKS

Today's Elementary Particles

Today's picture of the most elementary particles is composed of six quark types, six lepton types, and four force carriers. The quarks and leptons come in three generations, each generation with a pair of quarks (one with charge + 2/3, and one with charge - 1/3) and a pair of leptons (one charged, and one neutral). See Table 1. The quarks and leptons have spin 1/2, and couple variously to the spin 1 force carriers: gluons, photons, and charged and neutral weak bosons (W^+, W^-, and Z). Unlike the leptons, the quarks appear to come in three varieties, called colors. Perhaps the number of colors is related to the quarks' third-integer charges. Also, quarks never appear in isolation, being permanently confined, for example, in meson and baryon combinations (quark-antiquark and three-quark combinations, respectively).

These quark, lepton, and force-carrying particles are the foundation of the so-called Standard Model of particle physics. It is widely and completely accepted by the community. However, it was not always that way. The acceptance of the quark

TABLE 1. Today's elementary particles, by type vs generation.

Type	charge	1^{st} Generation	2^{nd} Generation	3^{rd} Generation
up-type quarks	+ 2/3	u up	c charm	t top
down-type quarks	- 1/3	d down	s strange	b bottom
neutral leptons	0	ν_e e neutrino	ν_μ μ neutrino	ν_τ τ neutrino
charged leptons	-1	e electron	μ muon	τ tau

picture of elementary particles owes a great deal to the discovery and understanding of the heavier quarks. Quarks were unexpected, even not accepted when I was a student. The idea of "partons" obeying SU(3) symmetry [1–3] was a mathematical tool at best, not a physical reality! [4] There were alternate possibilities for underlying structure; e.g., based on shapes, on how things are put together, and on the "bootstrap" model. [5] Perhaps the hadrons we see in the laboratory are each made of combinations of all the others, with no special subset being the most elementary.

The first confirmation of the idea of quarks came after the prediction by Murray Gell-Mann [4] of what we call the omega minus, understood now to be a baryon made of three strange quarks. This otherwise unheralded particle, was discovered in a 1964 Brookhaven bubble-chamber experiment headed by Nick Samios. [6]

The Revolution of November, 1974

The real watershed in thinking began with the announcement in November, 1974, that teams of physicists had observed a rather narrow resonance at a mass of 3.1 GeV/c^2. The resonance was seen in both hadroproduction [7] and e^+e^- annihilation. [8] The resonance still carries the dual name J/ψ from these concurrent observations. The quickly-accepted model explaining this narrow resonance was that it is made up of a new quark-antiquark pair. These new quarks were characterized by a new quantum number, called "charm." The existence of a new quark implied a whole spectrum of new particles containing at least one charm quark. Examples of these were soon discovered in e^+e^- collisions by the Mark I Collaboration at SLAC. [9]

The Growing Variety of Quarks

With the discovery of charm particles, there was a feeling that the quark picture of matter was complete, perhaps like the feeling at the beginning of the century when the atomic nature of matter was first understood. Nevertheless, only three

years after the discovery of charm, an even heavier resonance was observed in proton-nucleus collisions at Fermilab. [10] This resonance, at a mass of about 9.5 GeV/c^2 mass, was called upsilon, Υ, by it's discoverers. There was evidence in the initial data of some excited states of the ground-state resonance. These were quickly confirmed at DESY in Hamburg, [11] where the DORIS storage ring energy was boosted to be able to produce the new states. Thus, the bottom quark came to be an accepted member of the hierarchy of quarks.

As an aside, it might be noted that the τ, the charged lepton of the third generation, appeared just before the upsilon particle. The tau was not widely accepted, though it's discoverers were happy to see the upsilon as a confirmation that the earlier picture of two generations was incomplete. The tau was, then, also soon widely accepted. Direct observation of the tau neutrino has, by the way, also only just been announced this month.

A sixth quark was anticipated to be roughly 3 (or π) times the mass of the bottom quark. After all, there is such a pattern apparent among the strange, charm, and bottom quarks. The TRISTAN accelerator in Japan was even built with that goal in mind. However, in spite of major efforts, the discovery of the sixth, the "top" quark, did not occur until twenty years later, in 1997. The discovery required the dedicated running of the highest energy colliding-beams accelerator in the world, Fermilab's Tevatron Collider. This was because the top quark was not three times as heavy as the bottom quark, but about forty times as heavy; weighing in at about 175 GeV/c^2. The reason for this enormous mass remains a mystery.

As the number of quarks grew, another feature of quarks appeared. That is, the eigenstates relevant to their production in strong and electromagnetic interactions (called flavor eigenstates) are not the same as the weak-interaction eigenstates of their decay (called mass eigenstates). The various eigenstates mix, as related by the Cabibbo-Kobayashi-Maskawa (CKM) matrix. [12]

$$WeakEigenstates = \mathbf{V} \times FlavorEigenstates \tag{1}$$

That is,

$$\begin{array}{ccccccc} d' & & V_{ud} & V_{us} & V_{ub} & & d \\ s' & = & V_{cd} & V_{cs} & V_{cb} & & s \\ b' & & V_{td} & V_{ts} & V_{tb} & & b \end{array}$$

Using the Wolfenstein parameterization, [13] to order λ^3, the CKM matrix is

$$\mathbf{V} = \begin{array}{ccc} 1-\lambda^2/2 & \lambda & A\lambda^3(\rho - i\eta) \\ -\lambda & 1-\lambda^2/2 & A\lambda^2 \\ A\lambda^3(1-\rho-i\eta) & -A\lambda^2 & 1 \end{array}$$

The strong and electromagnetic interactions conserve the new quantum numbers, called "flavor:" strangeness, charm, bottom, and top. Thus, production of these

quarks in strong and electromagnetic interactions always occurs in pairs; i.e., a quark and an antiquark of the same flavor. This is the origin of the "strange" behavior of the strange particles – and of the heavier quarks which followed. On the other hand, the weak interactions do not conserve flavor. The violation of flavor conservation occurs in a well defined way, however, with the rates governed by the CKM matrix elements, V_{ij}, above.

A Few Comments on Names

The original names, up and down, came from an analogy with spinors, with spin direction pointing up and down. The "strange" quark name was chosen as a reminder that it was supposed to explain the strange behavior of particles containing these quarks; e.g., the K mesons which were always produced in pairs or in association with strange baryons. Stranger still, even with strange quarks, some neutral K meson decay behavior was not explained. The branching ratios to certain decay modes (e.g., $\mu^+\mu^-$) were much smaller than expected. One proposed solution, the GIM mechanism [14], suggested a fourth quark to fix things up. This fourth quark was to have just the right properties, be "charmed" in just the right way for the fix to work. The name "charm" was actually suggested earlier by Bjorken and Glashow in a paper generalizing SU(3) quark symmetry to SU(4). [15] I think that the name stuck, in part, because of the charmed properties of the quark. In any event, the mass of the charm quark was predicted on the basis of the needed properties for its cancellation of other contributions to the neutral K decays.

The third generation returned to more prosaic names, "top" and "bottom," like up and down, but not before flirting with the names "truth" and "beauty." I have preferred these latter names, since I used to describe my personal research as the "search for truth and beauty" – but that was before they were both discovered! This takes us to near the end of the current story. Let's review how the heavy quarks were first observed, their properties, and the basic physics associated with each of them.

EXPERIMENT TECHNIQUES LEADING TO HEAVY QUARK CAPABILITIES

Heavy quarks have been studied in a large number of experiments at quite a range of energies, from near threshold to much higher energies. Nevertheless, it will be evident as each heavy quark is discussed that certain experiment techniques have been critical to the success of the physics program. The same techniques appear and reappear. They will also be important for future physics efforts beyond heavy quarks.

The most important techniques for heavy quarks have been (1) efficient event selection, (2) long data-taking runs with lots of beam, (3) large data sets and lots

of computing, and (4) the use of solid-state detectors for precision charged-particle tracking. Each of these will be discussed in turn, though it is the combination of all of them together which has really made the difference.

Open, Efficient Event Selection

For charm, the first extensive open charm particle studies were done at e^+e^- colliders running at the ψ(3S), also called the ψ". Theses excited states of $c\overline{c}$ are produced copiously relative to an underlying continuum of states, and decay dominantly to $D\ \overline{D}$ mesons. Thus, experiments are able to record all the hadronic events in their studies of the D mesons. Final event selections are made later, off-line.

The early attempts to study charm particles at fixed-target experiments were less successful. They attempted to use special geometries for a single decay mode [16] and specialized triggers for particular production mechanisms [17]. Later experiments used looser event selection, and were more effective. Amid the generally-discouraging first efforts at fixed-target experiments, a list of algorithms was examined for event selection. [18] The more successful experiments made their event selections based on very open, efficient, inclusive triggers using total event transverse energy and evidence for decays of particles with lifetimes in the picosecond range. The first of these was effective to the extent that the new particles were heavy as a fraction of the center-of-mass energy, the second to the extent that the new particles had long lifetimes or decayed to particles with long lifetimes.

As was the case for charm, the first extensive studies of bottom particles were most successful at e^+e^- colliders. For bottom particles, the accelerators run at the energy where Υ(4S) particles are produced. Theses excited states of $b\overline{b}$ are produced copiously relative to an underlying continuum of states, and decay dominantly to $B\ \overline{B}$ mesons. Thus, experiments were again able to record all the hadronic events in their studies of the B mesons. The openness of the on-line event selection led to the ability of each experiment to attack a broad range of decays and of physics topics.

Even for the top quark discovery, the on-line trigger is quite efficient for top-quark events. The properties of the top quark are so extreme, that enormous numbers of less interesting events could be discarded at the on-line trigger level.

Large Data Sets and Lots of Computing

For each technique, technical progress has been critical to the extensive progress made in heavy-quark physics. In the case of data acquisition and analysis, the progress has been adopted from the commercial world where the cost per unit of data storage and computation has dropped amazingly over the last two decades. Table 2 lists the growth of charm samples achieved by increasing use of parallelism and computer power per CPU in one series of experiments, those at Fermilab's Tagged

Photon Laboratory. The basic experiment apparatus (a forward, two-magnet spectrometer) did not change much after the addition of silicon microstrip detectors in E691. Nevertheless, the number of reconstructed charm decays used in final physics publications grew exponentially. The physics signals shown in the table improve by a factor of 2,000, not counting the improvement in the signal-to-background ratio. Such numbers may be taken as a rough measure of the physics reach of the experiments.

The improved numbers of observed particles followed very nearly the increases in data set size, which was made affordable by the change from 9-track open-reel 6250 bpi magnetic tapes of E769 and earlier, to the use of 8 mm video tape in E791. A graphic demonstration of this difference is given by comparing the two images in Fig. 1. A fork lift and truck arrived at the E769 experiment each Monday morning to take the weekend's data tapes to the computing center. Compare that with nearly the same amount of data being held in the one arm-load of 8 mm tapes held by one of the E791 physicists. Perhaps even more impressive is the fact that the arm-load of tapes were filled with data in just three hours, not a full weekend. A similar growth of efficiency and cost effectiveness was needed in offline computing. It occurred via the use of "farms" of cheap, parallel, networked CPUs. [19] Table 3 gives the current status of the numbers of equivalent background free signals in some representative charm experiments, calculated from quoted signal sizes and their errors.

FIGURE 1. A forklift arrives at E769 (right) after a weekend of data taking using 9 track, 6250 bpi, open reel magnetic tapes. E791 physicist Cat James (left) holds an arm-load of 8 mm video tapes next to a storage rack of such tapes. An arm-load of tapes was filled in parallel by 42 tape drives in less than three hours.

TABLE 2. Example of the growth of computing parallelism and power from the series of charm experiments using the Fermilab Tagged Photon Spectrometer.

Time Frame	Exp. #	# Data Streams	# DAQ CPUs	# Output Streams	# Rec'd. Events ($\times 10^6$)	Data Set Size (Gbytes)	# Reconst'ed Charm Decays
1980-2	E516	1	1	1	20	70	100
1984-5	E691	2	1	1	100	400	10,000
1987-8	E769	7	17	3	400	1500	4,000
1990-2	E791	8	54	42	20,000	50,000	200,000

Silicon Microstrip Detectors and Charge-Coupled-Devices

Silicon microstrip detectors [20] (SMDs, shown in Fig. 2) and charge-coupled-devices (CCDs) provide very high precision information about the trajectories of charged particles. From these trajectories, we can obtain the locations where the trajectories overlap, e.g., the primary interaction point (primary vertex). Such a reconstruction from the charm photoproduction experiment E691 is shown in Fig. 3. We see a primary vertex and two secondary vertices where charm particles decay. Given the decay of the two long-lived particles near the primary interaction, the same tracking devices find the decay location as well as the primary vertex. How long lived must be the particles for these observations to be made in the laboratory? The time scale is a picosecond. A particle with such a lifetime will travel 300 microns in the laboratory if its velocity is such that $\beta\gamma$ is equal to 1.0.

TABLE 3. *Numbers of Equivalent Pure Decays Observed by Analysis (scaled to full data sets where needed).*

Physics Topic	Decay Mode	ALEPH	E791	CLEO II.V	FOCUS
Mixing	$D^o_{tag} \to K\pi$	1000	5,400	16,000	
	$D^o_{tag} \to K\pi\pi\pi$		3,300		
Mixing	$D^o_{tag} \to K\mu\nu$		750		7,400
	$D^o_{tag} \to Ke\nu$		760		
$\Delta\Gamma$	$D^o \to KK$		3,150	1,700	
	$D^o \to K\pi$		29,500	30,000	86,000
	$D^o \to K^o_s\phi$			4,100	
CP Vio.	$D^+ \to KK\pi$		1,250		8,100
	$D^+ \to \phi\pi$		800		
	$D^+ \to K^*(890)K^+$		420		
	$D^+ \to \pi\pi\pi$		590		
	$D^+ \to K\pi\pi$		36,000		120,000
CP Vio.	$D^o_{tag} \to KK$		440	2,100	2,200
	$D^o_{tag} \to \pi\pi$		190		
	$D^o_{tag} \to K\pi\pi\pi$		3,000		
	$D^o_{tag} \to K\pi$		10,500	13,500	35,000

This is only a little more than typical longitudinal position resolution values. So, experiments do best when the particles are traveling with higher velocities in the laboratory, and have larger values of $\beta\gamma$ – reaching values of a few tens even. For fixed-target experiments with incident charged-particle beams, one can also include the incident beam track and thin-target locations in fits to find the best estimate of the primary vertex location.

Use of the vertex information in an event provides a double benefit. First, events with evidence of a secondary vertex near the interaction point are highly enriched in heavy quark production. Once a decay vertex is located, the second benefit of precision tracking is evident. When searching for the right combination of observed particles from a single decay, one need only examine the effective mass of those particles coming from that decay vertex, not try all the combinations of all particles in the event. This reduces the backgrounds due to random combinations of tracks by very large factors.

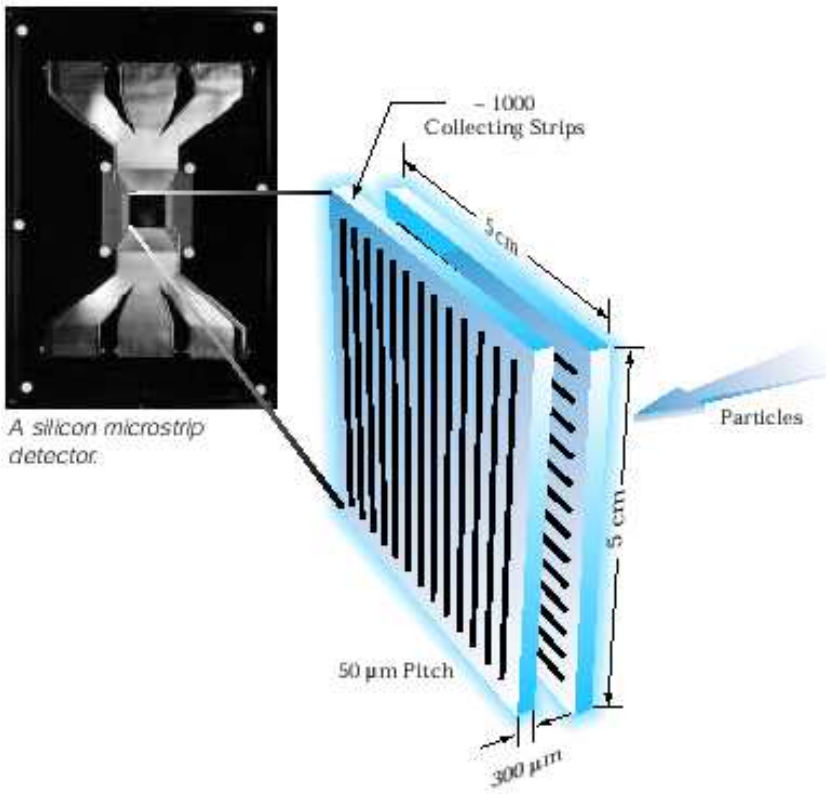

FIGURE 2. A silicon microstrip detector and sketch showing how orthogonal strips are used to map the trajectory of an incident charged particle. The solid-state detectors are fully depleted by application of a reverse bias across their 300 micron thickness, with signals of about 26,000 electrons observed.

OBSERVATIONS AND PHYSICS OF CHARM QUARKS

Observations of Charm

Although one long-lived event in cosmic rays [21] predated the observation of the J/ψ, it was the observation of the J/ψ in both hadronic and e^+e^- interactions that led to the wide acceptance of charm. The hadroproduction resulted in e^+e^- pairs seen in the experiment of Sam Ting and his group at Brookhaven. At SLAC, the group of Burton Richter saw a huge enhancement in the annihilation rate when the center-of-mass energy of the colliding e^+e^- beams was 3.1 GeV. Given that the J/ψ was made of a new quark-antiquark pair, a host of other new particles containing such quarks was expected. Among the new particles were excited states of the quark-antiquark pair. Some of these are listed in Table 4. These so-called charmonium states have no net charm, only "hidden charm." We also expected meson-combinations of charm quarks with lighter quarks and baryon-combinations with three quarks, one or more of which carried charm. The particles with net charm are known as "open charm" particles, and examples are listed in Table 5.

The early developments in charm physics were dominated entirely by experiments at e^+e^- colliders. The fraction of events with charm particles was large at the ψ". The backgrounds could be well handled for many decay modes, even though it was necessary to examine all combinations of tracks. Once silicon microstrip detectors were introduced into fixed-target experiments, combined with the other features discussed above, the most precise measurements came to be dominated by the Fermilab fixed-target program. Now, we can see the leadership position transferring to the asymmetric e^+e^- collider B factories. This is already evident in

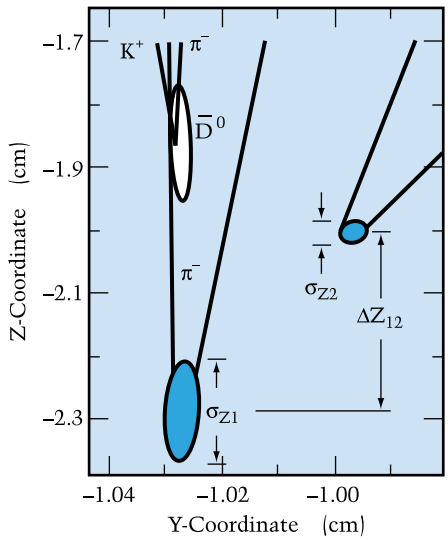

FIGURE 3. The reconstruction of vertices from trajectory information in an example E691 photoproduction event. The ovals represent the uncertainty in the vertex fits. Separation of the primary interaction and the decay points of two charm particles are clearly evident.

the preliminary results just announced at the ICHEP2000 Rochester Meeting held the previous week in Osaka, Japan. Perhaps, eventually, the lead will pass to the forward hadron-collider experiments at Fermilab and CERN – BTeV and LHC-b, respectively. Given the plans evident in the community today, future charm physics will come as a byproduct of the more intensive efforts aimed at understanding the b-quark system.

Techniques in Charm Experiments

The techniques discussed earlier used many charm experiment examples. They will not be repeated here. It is worth noting some additional features, nevertheless. Among these are the so-called D^*-trick, the use of the beam energy in making mass plots of charm candidates from ψ'' data, the use of additional kinematic and topological criteria, the use of high p_t leptons in triggers at fixed-target experiments, and charged particle identification as examples.

One special kinematic feature in charm is the very small kinetic energy available in the decay of the D^*, the first excited state of the D meson. This has been a useful feature, not only to find these D^* mesons in complicated environments like high-energy colliders, but also in selecting events where the nature at birth of the decay D^o is known. Thus, events with a π^+ which comes from a D^{*+} decay means that the accompanying D^o is not a $\overline{D}^o$. One can examine such events for evidence of mixing, that is if the D^o has become a $\overline{D}^o$ before it decays.

At e^+e^- colliders running at the ψ'', backgrounds are reduced and kinematic parameter resolution improves using the beam energy in making mass spectra distributions. The mass calculated this way is called the "beam constrained mass." The requirements used and the calculations are:

$$\Delta E = E_{candidate} - E_{beam} \tag{2}$$

and

$$M_{B\ candidate} = \sqrt{E_{beam}^2 - p_{candidate}^2} \tag{3}$$

In addition to looking for separations of decay vertices from the location of the primary interaction, one can demand for fully charged decay modes that the vector sum of the decay products point back to the primary vertex. This helps reduce backgrounds due to false combinations of reconstructed tracks. The technique even works, though less well, with a missing particle – especially if that particle is light as in the case of a missing neutrino. Of course, one must allow for some mismatch. One can also get to a two-fold-ambiguous momentum of a missing particle if one assumes the mass of that particle as well as the parent particle. The farther from the production point the decay is, the better this reconstruction performs.

TABLE 4. Examples of $c\overline{c}$ hidden-charm particles, their masses, widths, and typical decays.

J^{PC} Assignment	Symbol	Mass (MeV/c^2)	Width (MeV/c^2)	Decay Mode Examples
0^{-+}	$\eta_c(1S)$	2980 ± 2	$13.2^{3.8}_{3.2}$	$\eta\pi\pi$
0^{-+}	$\eta_c(2S)$ η_c'			not observed
1^{--}	$J/\psi(1S)$	3096.87 ± 0.04	0.087 ± 0.005	$2(\pi^+\pi^-)\pi^o$
1^{--}	$\psi(2S)$ ψ'	3685.96 ± 0.09	0.277 ± 0.031	$J/\psi(1S)\pi^+\pi^-$ $J/\psi(1S)\pi^o\pi^o$
1^{--}	$\psi(3S)$ ψ'''	3769.9 ± 2.5	83.9 ± 2.4	$D\overline{D}$
0^{++}	$\chi_{c0}(1P)$	3415.0 ± 0.8	$14.9^{2.6}_{2.3}$	$2(\pi^+\pi^-)$
1^{++}	$\chi_{c1}(1P)$	3510.5 ± 0.1	0.88 ± 0.14	$\gamma J/\psi(1S)$
2^{++}	$\chi_{c2}(1P)$	3556.2 ± 0.1	2.0 ± 0.2	$\gamma J/\psi(1S)$

Spectrum of Charm Mesons and Baryons

The first particles containing charm quarks to be observed were the so-called "onium" states of a charm quark and charm antiquark. These states have no net "charm," and can decay electromagnetically and, for the heavier such states, strongly. Thus, widths of the lower mass states are very narrow, and signals appear clearly above background. On the other hand, such states have unmeasurable decay lengths in the laboratory, making some observations difficult, if not impossible. Some of the observed charmonium states are listed in Table 4. Study of the charmonium states is still an active area. The η_c', for example, has not had a confirmed observation yet, in spite of several attempts. In addition, there are many more excited states of these onium particles.

It is the ground states with open charm that have longer lifetimes, and have been amenable to selection via their observable laboratory flight paths. The ground-state, open, single-charm mesons and baryons are listed in Table 5. No baryons with two charm particles among their three quarks have yet to be observed, though they should certainly appear eventually. Each of the ground-state particles can have a set of excited states, due either to radial or angular-momentum excitations. Many of these have already been observed, and there is a long story to be told here. Let me just note that these states are well described by focusing on the heavy charm quark as defining the coordinates, with an antiquark or diquark system orbiting around it. Spectrum mass-level separations agree with predictions from lattice gauge QCD calculations, and one can now even obtain values for the strong coupling constant from the level splittings in these states.

TABLE 5. Examples of open-charm particles and their decays.

Quark Combination	Symbol	Mass (MeV/c^2)	Lifetime (fs)	Decay Mode Examples
$c\overline{d}$	D^o	1864.5 ± 0.5	413 ± 2.8	$K^-\pi^+, K^-\pi^-\pi^+\pi^+$
$c\overline{u}$	D^+	1869.3 ± 0.5	1051 ± 1.3	$K^-\pi^+\pi^+$
$c\overline{s}$	D_s^+	1968.6 ± 0.6	496^{+10}_{-9}	$K^-K^+\pi^+$
cud	Λ_c	2284.9 ± 0.6	206 ± 12	$pK^-\pi^+$
cuu	Σ_c^{++}	2452.8 ± 0.6		$\Lambda_c^+\pi^+$
cud	Σ_c^+	2453.6 ± 0.9		$\Lambda_c^+\pi^o$
cdd	Σ_c^o	2452.2 ± 0.6		$\Lambda_c^+\pi^-$
csu	Ξ_c^+	2466.3 ± 1.4	330^{+60}_{-40}	$\Lambda K^-\pi^+\pi^+$
csd	Ξ_c^o	2471.8 ± 1.4	98^{+23}_{-15}	$\Xi^-\pi^+, \Omega^-K^+$
css	Ω_c	2704 ± 4	64 ± 20	$\Sigma^+K^-K^-\pi^+$

Physics Issues for Charm Quarks

The physics issues for charm quarks range from searches for clues to new physics to contributions to the understanding and parameters of the Standard Model. The searches for physics beyond the Standard Model include those which would appear as CP violation, oscillations between neutral states, and searches for forbidden and overly copious rare decays. Among the Standard Model parameters to be measured accurately are the CKM matrix elements: $|V_{cs}|$ and $|V_{cd}|$, determination of the strong coupling constant α_s as a test of the flavor independence of QCD, branching ratios and lifetimes to high precision, and a myriad of resonance and other non-perturbative parameters.

Charm, a Unique Window to New Physics

Two features of charm make it unique in the search for new physics: (1) the absence of Standard Model background and (2) the fact that coupling to charm is the only way to see new physics in the up-quark sector. The Standard Model sources of mixing and CP violation for strange and bottom quarks predict significant, even large effects. Yet, for charm, such effects are predicted (so far) to be unmeasurable. Thus, experimental signatures in charm have no SM background, no relevant hadronic uncertainty in background estimates. Any sign of mixing or CP violation in the charm sector is immediate evidence of new physics. [22,23]

As for new physics coupling to the up-quark sector, both the up-quark and the top-quark are prevented from having observable effects in virtually all the standard ways of looking. There is a lack of decay channels for the up quark itself. So, interferences among decay channels are severely constrained. The top quark doesn't live long enough to mix or have the final state interactions needed for CP violation.

Mixing in the Standard Model is a good example of why effects are so small in the charm sector. The Standard Model process is thought to be dominated by contributions of the so-called "box diagram" shown below. Down-type quarks appear

in the loop for this mechanism. The amplitude has the form

$$A_{mix}(\text{charm box diagram}) \sim (m_s^2 - m_d^2)/m_W^2 \times (m_s^2 - m_d^2)/m_c^2 \tag{4}$$

where the first term comes from the sum of the two leading terms (GIM suppression), and the second is an off-shell factor. In the limit of SU(3) symmetry, the down and strange quarks have equal masses and the amplitude is zero. Comparing

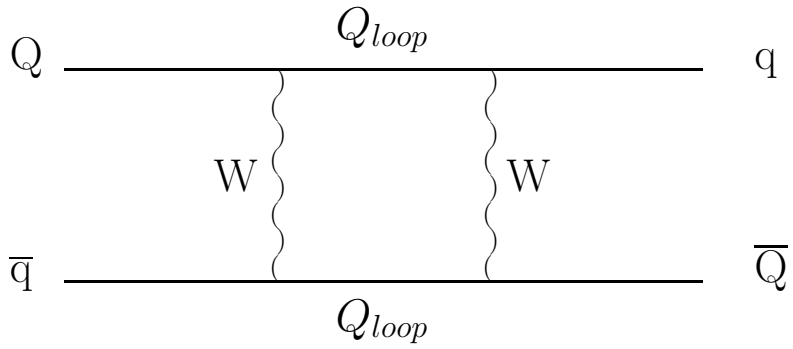

Q = c – Q_{loop} = b,s,d
Q = s,b – Q_{loop} = t,c,u

this to the same sort of diagram for mixing of neutral kaons with up-type quarks in the loop shows the orders-of-magnitude difference due to the coupling constants (CKM parameters) and the masses of the quarks involved.

$$A_{mix}(\text{kaon box diagram}) \sim (m_c^2 - m_u^2)/m_W^2 \times (m_s^2 - m_d^2)/m_s^2. \tag{5}$$

Note that for neutral kaon decays to dileptons to be as small as they are, the cancellation of the charm and up quark contributions is required in such loop diagrams. This is what allowed Glashow, Iliopoulos, and Maiani to predict the mass of the charm quark before there was any direct evidence for it. Contributions from these box diagrams, and even those from penguin and long distance effects are of the order of 10^{-7} to 10^{-10}. A rather complete compilation of model-dependent calculations for both Standard-Model and new-physics models is being maintained by Harry Nelson. [24]

We often refer to the gap between Standard Model backgrounds and the current level of experiment limits as an open window. That is, there is an opening for a major discovery. Table 6 lists a number of measurements, the current levels of sensitivity, and the theoretical estimates of the contributions of Standard Model

sources to possible signals. There are orders of magnitude available in these open windows. Furthermore, there are many extensions of the Standard Model which might appear in the window. These include fourth-generation quarks, leptoquarks, and various other heavy particles (e.g., Higgs and SUSY particles) which can appear in loops in virtual processes.

Charm Production - Cross Sections

The charm cross section is relatively small for fixed-target photoproduction, where charm is produced in only about a half percent of hadron-producing interactions. The charm cross section is even smaller in fixed-target hadroproduction, where charm is produced only about once per thousand interactions. Once one gets to Tevatron Collider energies, the fractional cross sections rise by an order of magnitude.

The theoretical uncertainties associated with charm hadroproduction predictions are about an order of magnitude at fixed-target energies, even for next-to-leading-order calculations. This is due to the sensitivity to the charm quark mass and the scale dependence of these calculations. In principle, calculations for production at very high transverse momentum might mitigate the scale dependence, but this has yet to be observed. Calculations for photoproduction have somewhat less uncertainty.

The charmonium production is a small fraction of total charm hadroproduction. The comparison with calculations for the J/ψ and ψ' are complicated by the existence of sources like bottom decay and the decay of the higher excited charmonium states. Nevertheless, the levels of these sources have been measured. Once these are subtracted, a mystery remains. At both fixed-target and collider energies, the direct production J/ψ and ψ' mesons are measured to be factors of 7 and 25 larger, respectively, than predicted by the simple color-singlet model. When this is "explained" by including color-octet contributions, the hadron-collider matrix elements are not consistent with the levels observed at the HERA ep collider.

Charm Production - Hadronization Effects

The process of produced charm quarks turning into the charm mesons and baryons observed in the laboratory is called hadronization. The process is non-perturbative by its very nature. Nevertheless, some patterns are emerging. For one thing, the longitudinal momentum of observed charm mesons in hadronic interactons looks very much like the predicted distribution calculated for quarks. This appears to come about because of a cancellation of "color drag" and fragmentation. The first of these is an acceleration of the produced quarks in the direction of the incident particles. This is said to be due to the pull of the color strings which attach the charm quark to the forward-going remnants of the incident particle. The fragmentation is the deceleration of the charm quarks as they pick up sea-quarks

TABLE 6. Exmples of the Open Window Sensitivity to Physics Beyond the Standard Model.

Topic	90% CL Limit	SM prediction	Typical Models Tested
CP Violation			
$D^0 \to K^-\pi^+$	-0.009<a<0.027 [25]	≈ 0 (CFD)	SUSY,
$D^0 \to K^-\pi^+\pi^-\pi^+$		≈ 0 (CFD)	LR Symm.,
$D^0 \to K^+\pi^-$	-0.43<a<0.34 [26]	≈ 0 (DCSD)	Extra Higgs
$D^+ \to K^+\pi^+\pi^-$		≈ 0 (DCSD)	
$D^0 \to K^-K^+$	-0.026<a<0.028 [27]		
	-0.093<a<0.073 [28]		
	-0.022<a<0.18 [25]		
$D^0 \to \pi^+\pi^-$	-0.002<a<0.094 [27]		
	-0.186<a<0.088 [28]		
$D^+ \to K^-K^+\pi^+$	-0.006<a<0.018 [27]		
	-0.026<a<0.028 [29]		
$D^+ \to \overline{K}^{*0}K^+$	-0.092<a<0.072 [29]	$(2.8\pm0.8)\times10^{-3}$ [31]	
$D^+ \to \phi\pi^+$	-0.075<a<0.21 [30]		
$D^+ \to \pi^+\pi^+\pi^-$	-0.086<a<0.052 [29]		
$D^+ \to \eta\pi^+$		$(-1.5\pm0.4)\times10^{-3}$ [31]	
$D^+ \to K_S\pi^+$		few $\times10^{-4}$ [32]	
FCNC			
$D^0 \to \mu^+\mu^-$	4×10^{-6} [33,34]	$< 3\times10^{-15}$ [35]	4^{th} Gen.,
$D^0 \to \pi^0\mu^+\mu^-$	1.7×10^{-4} [36]		Tree-level
$D^0 \to \overline{K}^0e^+e^-$	1.1×10^{-4} [37]	$< 2\times10^{-15}$ [35]	FCNC
$D^0 \to \overline{K}^0\mu^+\mu^-$	2.6×10^{-4} [36]	$< 2\times10^{-15}$ [35]	
$D^+ \to \pi^+e^+e^-$	6.6×10^{-5} [38]	$< 10^{-8}$ [35]	
$D^+ \to \pi^+\mu^+\mu^-$	1.8×10^{-5} [38]	$< 10^{-8}$ [35]	
$D^+ \to K^+e^+e^-$	2.0×10^{-4} [39]	$< 10^{-15}$ [35]	
$D^+ \to K^+\mu^+\mu^-$	9.7×10^{-5} [39]	$< 10^{-15}$ [35]	
$D \to X_u + \gamma$		$\sim 10^{-5}$ [35]	
$D^0 \to \rho^0\gamma$	2.4×10^{-4} [40]	$(1-5)\times10^{-6}$ [35]	
$D^0 \to \phi\gamma$	1.9×10^{-4} [40]	$(0.1-3.4)\times10^{-5}$ [35]	
LF or LN Violation			
$D^0 \to \mu^\pm e^\mp$	8.1×10^{-6} [41]	0	LQ
$D^+ \to \pi^+\mu^\pm e^\mp$	3.4×10^{-5} [41]	0	
$D^+ \to K^+\mu^\pm e^\mp$	6.8×10^{-5} [41]	0	
$D^+ \to \pi^-\mu^+\mu^+$	1.7×10^{-5} [41]	0	
$D^+ \to K^-\mu^+\mu^+$	1.2×10^{-4} [41]	0	
$D^+ \to \rho^-\mu^+\mu^+$	5.6×10^{-4} [36]	0	
Mixing			
$^{(}\overline{D}^{)0} \to K^\mp\pi^\pm$	$\Delta M_D < 2.8\times10^{-5}$ eV [26]	10^{-7} eV [22,42]	LQ, SUSY,
$^{(}\overline{D}^{)0} \to K\ell\nu$	$r < 0.005$ [43]		4^{th} Gen., Higgs

to make observable particles. There is some evidence for the attachment of color strings to the charm and valence quarks of projectiles. This is called the "leading particle" effect. In this effect, we see an asymmetry in the forward direction in the numbers of particles with valence quarks in common with the projectile compared

to those without. For example, in incident negative-pion-beam experiments, there is a preponderance of D^-'s over D^+'s. For kaon beams, the preponderance is of D_s mesons with the same strange quark as the valence strange quark in the incident kaons.

The details of the production process are also probed by measurements of the correlations of charm and anti-charm particles. One mystery here is why the charm and anti-charm particles do not appear more nearly back-to-back in the plane transverse to the incident particle. Some smearing can come from the intrinsic transverse momentum, k_t, of the partons in the incident particles. However, the amount of k_t required to explain observations in hadroproduction can be as much as 2 to 3 GeV/c. This is rather large, even for a nucleon whose total rest mass is on the order of 1 GeV/c^2.

Charm-Particle Lifetimes

The lifetimes of charm particles would all be the same if they all were the result of a single process, say the color-aligned spectator diagram where the charm quark decays to the Cabibbo-favored W^+ and a strange quark, with the W^+ becoming some final state particle via its virtual decay to $u\overline{d}$. However, there are other possibilities: an annihilation diagram, a W-exchange diagram, and a second (color suppressed) spectator diagram where the quarks from the W decay do not stay together.

Various of the mesons and baryons have differing contributions from each of these diagrams. From the lifetimes listed in Table 5, it is evident that more than a single process must be relevant. Lifetimes of the ground-state charm particles vary by an order of magnitude! A consistent picture of charm decay requires inclusion of all these processes, including coherent interference of diagrams when the final-state particles from two diagrams are the same. [44] There is also evidence of enhancement of the hadronic modes by diagrams with gluons. [45] This gluon participation may account for the fact that the color-suppression in charm decay is not as pronounced as in bottom decays.

Charm Decay - Resonance Dominance and Light Resonance Parameters

Detailed study of the decays of charm mesons and baryons shows a dominance by quasi-two-body modes, that is where the charm particle decays to a low-mass hadron resonance and another particle. The study of such decays is often pursued by examining the distribution of decays in terms of their Dalitz plot, the two-dimensional distribution for three particles in the final state which is uniform for non-resonant s-wave decays, and has various structures evident for other modes. An example is the Dalitz plot for $K\pi\pi$ decay of the D^+ meson shown in Fig. 4. Each dot represents a measured decay; it's location in the plot is a function of the location in the available decay phase-space.

The plot is a beautiful demonstration of basic physics, for example that observations are driven by the square of the more fundamental amplitudes. We see that in the distinct interference pattern between the $K^*(890)$ resonance, observed as a band at the K^*-mass squared, and the more slowly varying other decay contributions. We also see the conservation of angular momentum in this decay of a pseudoscaler particle into a vector particle, the K^*, and a pseudoscalar, the recoiling pion in the decay. This combination of spins, leads to a $(1 + cos(\theta))$ decay angular distribution, which shows up in the Dalitz plot as a concentration of K^* events near the kinematic boundary. Thus, we see that the distributions in the Dalitz plot are characteristic of the resonances involved and their masses, widths, and spins.

As is evident from this one Dalitz plot example, the distribution is sensitive to which resonances contribute to the decay, the mass and width of those resonances, and to the relative phase of the contributions of the decay. Much of the information on low-mass resonances has come from scattering experiments. There, the partial

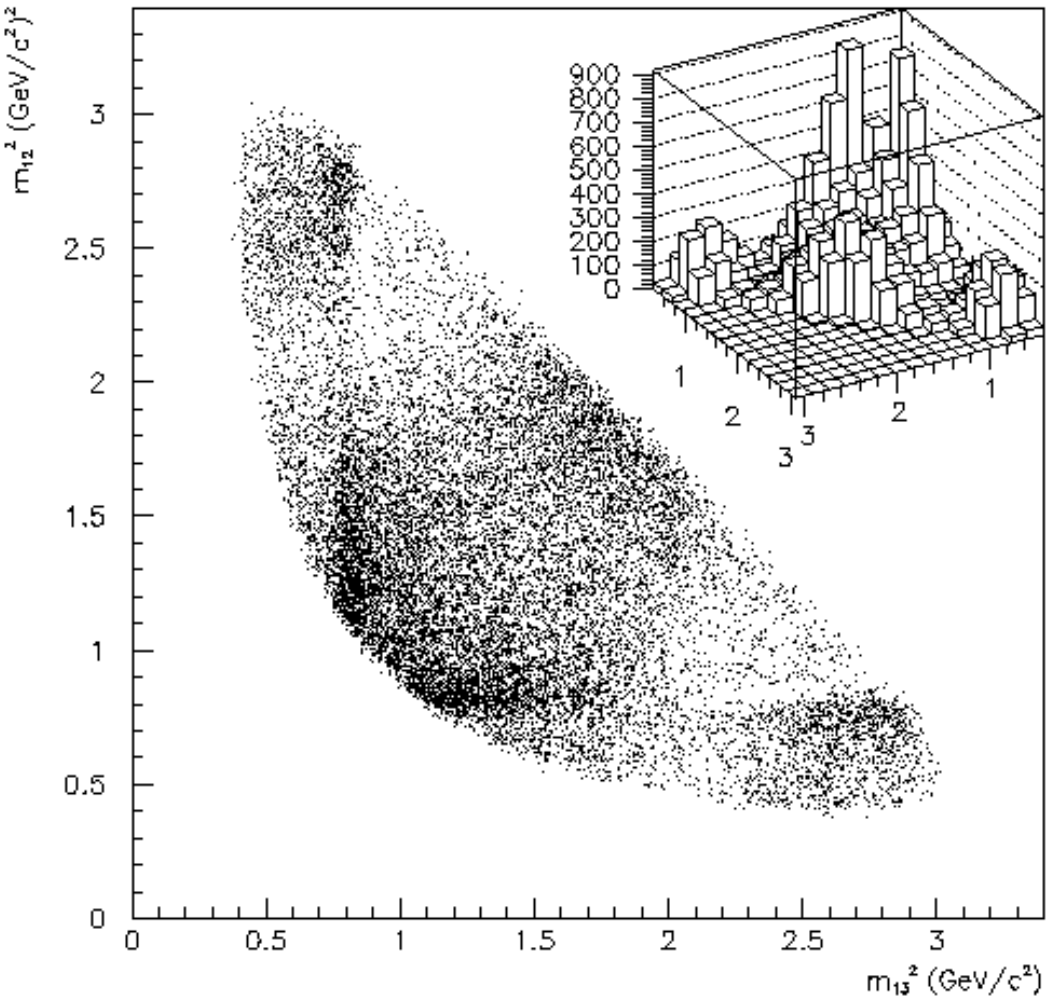

FIGURE 4. The Dalitz distribution for the decay $D^+ \to K^-\pi^+\pi^+$. Since the two pions are indistinguishable, the data has been symmetrized in making the figure.

waves which contribute can be quite complex. In the decay of charm particles, the initial state is somewhat better defined, less complex. Thus, charm decay can be used as an independent way of understanding light-resonance physics.

One of the most compelling examples of this is in the three charged pion decays of the D^+ and D_s^+ mesons. In these decays, one observes the contributions from such final states as $\rho^o\pi^+$, $f_o(980)\pi^+$, $f_2(1270)\pi^+$, $f_o(1370)\pi^+$, $\rho^o(1450)\pi^+$, and $\sigma\pi^+$. The decays are dominated by the scalar plus π^+ modes, and the initial quark content of the D's and that of the resonances can be understood to be consistent. This latter point is useful in determining the decay mechanisms at work (e.g., what fraction of the decays come from the annihilation diagram) and the nature of some of the less-well understood resonances such as the $f_o(980)$, the $f_o(1270)$, and the σ. The parameters of these resonances have been determined from the fits to the relevant Dalitz distributions. Although it is not so clear from Fig. 4, a very large part of the slowly varying density of decays comes from the scalar κ resonance. It's mass and width are being determined in a new result from E791. [46]

Study of the Dalitz plots of charm particles can also help in untangling the contributions of the basic quark-level decay diagrams. Various resonances are characteristic of different decay mechanisms for a given charm parent. So far, the contributions of non-spectator diagrams for mesons appears to be somewhat limited. However, baryons have a richer set of possibilities since helicity is no longer a supressing factor. In fact, the variety of baryon lifetimes can be explained by incorporating the variety of possible quark-level diagrams.

Summary of Charm Physics

We have gone very quickly over the enormous range of physics topics where charm quark experiments can contribute. These included (1) new physics searches, (2) Standard Model electroweak parameters, and (3) QCD understanding and parameters in production, spectroscopy, and decay mechanisms.

OBSERVATIONS AND PHYSICS OF BOTTOM QUARKS

As in the case of charm quarks and their physics, I will briefly review the first observations of bottom, the types of experiments which have studied bottom particles, the particular techniques used, and finally the range of physics topics of special interest for bottom.

Observations of Bottom Quarks

The first observation of bottom quarks was in a 1977 fixed-target hadroproduction experiment at Fermilab. There, the group headed by Leon Lederman observed $\mu^+\mu^-$ pairs in a complicated peak near a mass of 9.5 GeV/c^2 above a continuum. [10] The experimenters, conscious of the resonances in the J/ψ system, recognized that they might be seeing such a system for a new, third generation quark. The Fermilab

TABLE 7. Examples of open-bottom particles and their decays.

Quark Combination	Symbol	Mass (MeV/c^2)	Lifetime (fs)	Decay Mode Examples
$\overline{b}d$	B_d or B^o	5279 ± 2	1548 ± 32	$D^-\pi^+\pi^+\pi^-$
$\overline{b}u$	B^+	5279 ± 2	1653 ± 28	$D^o\rho^+$
$\overline{b}s$	B_s	5369 ± 2	1493 ± 62	$D_s^- X$
$\overline{b}c$	B_c	6400 ± 430	460^{+180}_{-160}	$J/\psi\pi^+$
bud	Λ_b	5624 ± 9	1229 ± 80	$J/\psi\Lambda$

results led to an energy upgrade of the DORIS e^+e^- collider at DESY in Hamburg, Germany. There, several experiments were able to offer rather quick confirmation of the discovery. [11] Because of the much better mass resolution based on beam energies at DORIS, the experimenters were able to discern three resonances, just where the Lederman group had said they were.

Spectrum of Bottom Mesons and Baryons

Similarly to the case of charm, but with an even greater potential variety of particles, the bottom system observations are all consistent with the pattern expected for the usual meson and baryon quark combinations. Table 7 gives examples of the better known particles. Many others are anticipated, but have yet to be observed. There are also many states of hidden "beauty," not shown, and of radial and angular-momentum excitations of all the ground states. Even for the observed particles, however, the full demonstration of their expected spin and parity has yet to be accomplished.

Special Techniques Used for Bottom

Particles containing bottom quarks have been observed in a great variety of experiments, from threshold to very high energies – more so than any of the other heavy quarks. At symmetric e^+e^- colliders such as CLEO at Cornell, the machines are operated at the $\Upsilon(4S)$ where the resonance is just above $B\overline{B}$ threshold. Thus, since the center of mass is nearly at rest in the laboratory, the B's are also nearly at rest in the laboratory. In order to produce B's with significant laboratory lifetimes, Pier Oddone and collaborators proposed building an asymmetric e^+e^- collider. [47] At such a machine, since one beam has higher energy than the other, the center of mass is moving in the laboratory. Thus, the Υ(4S) and its decay B's are moving in the laboratory. In this environment, the observation of isolated secondary vertices is again a most useful tool. Two major facilities of this sort have just turned on successfully, and the experiment at each facility has reported its first physics results at the ICHEP 2000 meeting in Osaka, Japan. The experiment is called BaBar at the PEP-II machine at SLAC, and BELLE at the KEK-B machine in Japan.

At fixed-target experiments, where the b was first discovered, the available energy is not as well controlled as at e^+e^- colliders, but the typical energies also produce b's nearly at rest in the center of mass. However, because of the beam momentum,

the B's travel with several tens of GeV/c in the laboratory. Several experiments have observed bottom particles, especially the Υ and B-decays to J/ψ's. E288, E605, E653, E771, and E789 at Fermilab are described briefly in a commemorative book available on the web [48]. There are also HERA-B at DESY and BEATRICE (WA92) at the CERN SPS. Only HERA-B among all these is still in the data taking mode.

Much higher energy B's and b-baryons are seen at high-energy hadron collider experiments – e.g., CDF, and DZero already, and at LHCb, BTeV in the future. Here the bottom particles have significant lifetimes in the laboratory, making their observation easier – except that the b quarks often turn into full-scale jets of many particles, not just the pristine B's seen at lower energies. Symmetric e^+e^- colliders running at the Z^o mass and above have similar access to b physics, again with b's dominantly in jets of particles. We have seen interesting results from the SLD experiment at SLAC and four LEP experiments at CERN: ALEPH, DELPHI, L3, and OPAL.

Across this range of experiments, there are a few special techniques which come into play. At the e^+e^- colliders running at the $\Upsilon(4S)$, backgrounds are reduced and kinematic parameter resolution improves using the "beam constrained mass" – as was the case for charm from the ψ" experiments at e^+e^- colliders. In addition, at fixed-target experiments and within jets at higher energies, leptons with high p_t play a role, and visible lifetimes for open bottom mesons and baryons are again crucial.

In looking for mixing of neutral B mesons in hadronic interactions, it is again necessary to know the nature of the B at birth, as well as its nature when it decays. In the case of the e^+e^- colliders, the difference in the nature of the two B's as they decay is needed. This sort of knowledge is obtained by observing one B as it decays, and using information either about the other B in the event or about the produciton of the first B. Using partial information about the other B is called "tagging." Tagging usually involves incomplete knowledge, in order to have as many tagged events as possible. Thus, experimenters examine the net charge, weighted by momentum, or observed decay leptons from the other B or b-jet. For information about the fully reconstructed B, one can use information on its production angle when there is a strong asymmetry, as when highly polarized electron or positron beams are used at e^+e^- colliders operating at the Z^o with its weak decay asymmetry – so far only at the SLC facility at SLAC. At hadron colliders one can also examine other particles produced in the jet with the B. The most information is available when examining the single other particle nearest in phase space to the B. Detailed information about such production correlations is then needed to fully understand the tagging rate and backgrounds.

Physics Issues for Bottom Quarks

The bottom quark is part of a standard (left-handed) quark isospin doublet (b, t), although there were many early attempts of think of it as a singlet. The dominant b decay is to c quarks, via emission of a virtual W, a 3^{rd} to 2^{nd} generation transition. This coupling is much less strong than the s to u transition, a 2^{nd} to 1^{st} generation

transition. The coupling of the b to the u quark, 3^{rd} to 1^{st} generation, is even weaker. The GIM mechanism breaks down since the t quark is so massive. The massiveness of the t quark also leads to very large $B^o\overline{B}^o$ mixing. This was observed very early via a surprisingly large same-sign di-lepton signal, [49] though it was not so widely accepted at first. It was the first indication that the top quark was so extraordinarily heavy.

Today, there are extensive efforts to measure the parameters of the B meson system. While we refer to this as being done to test the Standard Model, most hope that we will find evidence for physics beyond the Standard Model – that is, evidence that there is no single set of parameters within the Standard Model that can explain all observations. Thus, it is important to observe each parameter in more than a single way. This is often called overdetermining the CKM matrix. Experiments are focusing on:

CP violation

Oscillations in neutral states, both B_d and B_s

Rare and nominally-forbidden decays

There are still issues in the details of decay dynamics, since there are discrepancies between expectations and some lifetime measurements. An additional wrinkle in the picture is the relationship between the semileptonic decay rate and the number of charm particles observed in b decay. The semileptonic decay rate is 1 to 2% below the rate (more like 12%) expected from theory using standard CKM matrix elements. Considering $b \to W^-c$ and W^-u, with $W^- \to \overline{u}d$, $\overline{c}s$, $e^-\overline{\nu}_e$, $\mu^-\overline{\nu}_\mu$, and $\tau^-\overline{\nu}_\tau$, the semileptonic branching ratio should be $\sim 1/9$, given 3 colors for the quarks. Phase space for c and t quarks and final state interactions for $W \to$ quarks modify this somewhat.

In addition to the electroweak theory which is the main part of the Standard Model being tested above, there are also issues for QCD. The flavor independence of the strong coupling constant has been established by looking at the rate of gluon emission in e^+e^- interactions involving the light, the charm, and the bottom quark. One might expect that the bottom quark is heavy enough that NLO perturbative QCD would suffice to explain b quark production. However, again there are mysteries to be unraveled here. The importance of the hadronization process for tagging has been mentioned already.

Bottom Production - Cross Sections

Given that the b mass is much larger than Λ_{QCD}, the expectation is that NLO perturbation theory will reliably predict $\sigma_{b\overline{b}}$. At the Tevatron Collider, where the high transverse momentum of the observed B's should also help, the measurements give $\sigma_{b\overline{b}}$ too large by a factor at least two. [50,51]

The CDF and DZero measurements at the Tevatron are dominantly in the central region of phase space. This will also be true for the LHC experiments ATLAS

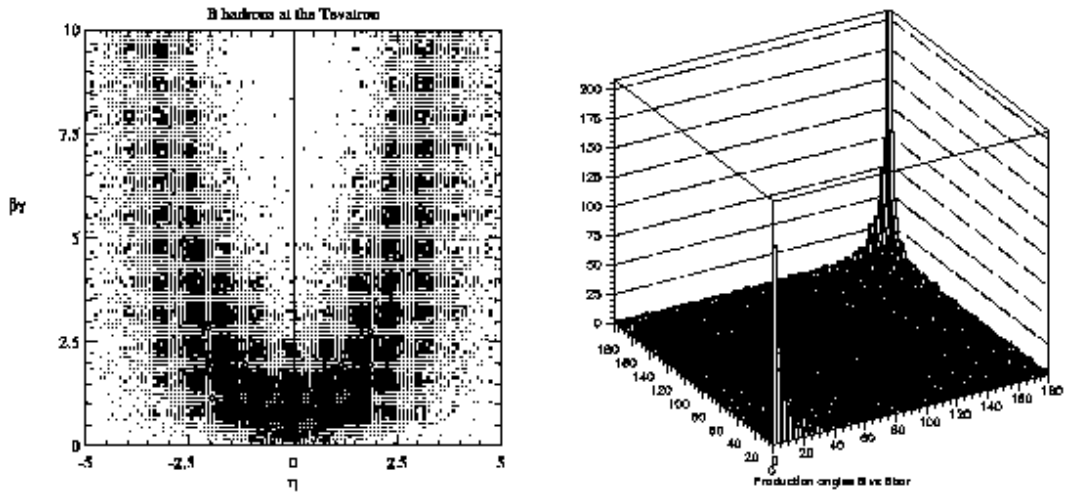

FIGURE 5. Distributions of b and $\overline{b}$ produced in interactions at the Tevatron Collider. On the left is the time dilation factor $\gamma\beta$ vs the pseudorapidity, on the right is the angular correlation of b and $\overline{b}$ quarks.

and CMS. However there are two new experiments which will explore the forward regions, BTeV at the Tevatron and LHC-b at the LHC. These latter experiments will take advantage of the higher momentum and longer laboratory lifetimes of bottom particles in their kinematic region. See the left side drawing of Fig. 5. Also shown in Fig. 5 is the strong correlation in produciton of the b and $\overline{b}$ in the forward and backward directions predicted by the PYTHIA simulation model. This appears as the strong peaking in the number of events shown on the figure on the right side of Fig. 5. BTeV and LHC-b should be able to take advantage of this correlation in tagging the B's which they will observe.

Bottom Production - Hadronization Effects

Bottom quarks turn into B mesons which decay to charm. The charm distributions depend on the fragmentation (hadronization) functions for the b quarks, the harder the B meson, the harder the charm. Examples are the

Andersson function:

$$\phi(z) \sim z^{-1}(1-z)^a e^{-bm_t^2/z} \tag{6}$$

and the Peterson function:

$$\phi(z) \sim 1/[z[(1-(1/z)-\epsilon_P/(1-z)]^2] \tag{7}$$

The CLEO Collaboration has looked at D_s decays of B mesons as a particularly clean way to determine the best parameters and relative merits of these two functions. [52] These distributions are important in understanding experiment apparatus acceptance and in determining backgrounds for top quark and other heavy objects. Yet, we may ask whether the fragmentation functions from e^+e^- are relevant in hadronic environments? [53] If they may be so at high p_t where approximate

isolation may be achieved, how low can one go in p_t before the color-field environment is so different that the e^+e^- measurements are not applicable.

Bottom-Particle Lifetimes

The original expectations for bottom particles was that their lifetimes would be short, even with a new quantum number to conserve, because of the large phase space and multitude of decay modes available. However, it turned out that the CKM-matrix parameters were small, thus leading to long lives. As with charm, the expectation was for equality of lifetimes – all ~ 1.5 picosecond. However, as seen in Table 7, there are significant differences. The shortness of the Λ_b lifetime is particularly difficult to explain.

Neutral Bottom-Particle Mixing

Both B_d and B_s particles are expected to have observable mixing. However, the rate of B_s oscillation will be very much more rapid, and correspondingly harder to measure. B_d mixing has been observed by several experiments, in a number of ways – even directly. No B_s mixing has yet been seen. This mixing is expected to lead to CP violation due to the phase in the CKM matrix (i.e., a non-zero value of ρ in Eq. 1).

Additional Bottom Decay Issues

The very hot topic in bottom particle decays is CP violation in B meson decay. The idea is to test the Standard Model prediction for the violation – in the hopes of finding a disagreement which would provide a clue to physics beyond the Standard Model, just as that is the hope in studies of charm decay. We anticipate that very heavy particles may make virtual contributions to the box diagrams in a measureable way. Non-Standard Model "penguin" decay diagrams also are open to virtual particles; e.g., heavy W and charged Higgs in place of the traditional W in loops. See the lectures at this workshop by Gabriel Lopez, "Violación de CP en Mesones B," for more on this subject.

Among the things which complicate experimental work in bottom decays is the large number of decay channels available for each bottom particle. This leads to very small BR's (typically very much less than 1 %) and the difficulty of collecting large samples of a given decay mode. Yet, this is exactly what is needed for high precision measurements and searches; e.g., searches for small CP asymmetries. It is usually the case that the largest such asymmetries are anticipated for the smaller branching-ratio decay modes. Furthermore, only a fraction of the decay channels have actually been observed.

OBSERVATIONS AND PHYSICS OF TOP QUARKS

Again, for the heaviest of quarks, the top quark, I will review its first observation, the techniques used, the measurements made, and make a rapid tour through the physics issues related directly to top quarks.

First Observations of Top Quarks

The discovery of top quarks required seeing interactions with the characteristics expected, and at a rate greater than that which could be expected from other processes. The signal for top quarks so far does not stand out quite as clearly as the signals for charm and bottom quarks did. Given their very high mass, top quarks could only be discovered in proton-antiproton collisions at the 1.8 TeV center-of-mass energy available at Fermilab's Tevatron. Furthermore, the signals appear near the end of the spectra where the rates are low. The cross section turns out to be about $5pb^{-}1$. This corresponds to one such event produced in about 2×10^{10} events.

Observation of the top quarks has depended on the high mass of the top quark, and the high mass and p_t of its decay products. Fortunately, the decay is completely dominated by a single mode:

$$t \to Wb$$

Three topologies result from $t\overline{t}$ production and decay: 6 jets, 4 jets plus a lepton, and 2 jets plus 2 leptons:

$$t\overline{t} \to [W^-\overline{b}]\ [W^+b] \to [(q\overline{q}')\ b]\ \ [q''\overline{q}''')\ \overline{b}]$$

$$t\overline{t} \to [W^-\overline{b}]\ [W^+b] \to [(\ell\overline{\nu}_\ell)\ b]\ \ [(q\overline{q}')\ b]$$

$$\text{and } [(q\overline{q}')\ \overline{b}]\ \ [(\overline{\ell}\nu_{\overline{\ell}})\ \overline{b}]$$

$$t\overline{t} \to [W^-\overline{b}]\ [W^+b] \to [(\ell\overline{\nu}_\ell)\ b]\ \ [(\overline{\ell}'\nu_{\overline{\ell}'})\ \overline{b}]$$

In order to optimize the observation above background, the experiments which made the observations, CDF and DZero, focused on central kinematic region. Most other processes are peaked forward-backward; and the high mass decay daughters benefit from the Jacobian enhancement perpendicular to the incident particles. Only events with very high p_t jets and leptons; and missing, high transverse energy E_t from neutrinos were examined. Furthermore, b-quark jet tagging via leptons and secondary vertices was very helpful. The largest backgrounds came from W plus low-mass q jets. So, the techniques used for bottom quark physics are directly relevant here for top quarks as well. Finally, kinematic constraints on the t-quarks and W^+ and W^- candidates were used. Though the t quark mass was unknown, both t's must have same mass; and W mass was known.

TABLE 8. Top Quark Production Cross Section Measurements.

$\sigma_{t\bar{t}}$ (pb)	Source	Ref.	Method	Total Events	Background Events
4.1 ± 2.0	DZero	[54]	lepton plus jets	19	8.7 ± 1.7
8.2 ± 3.5	DZero	[54]	lepton plus jets/μ	11	2.4 ± 0.5
6.3 ± 3.3	DZero	[54]	dileptons and $e\nu$	9	2.6 ± 0.6
5.5 ± 1.8	DZero	[54]	DZero combined	39	13.7 ± 2.2
$6.7^{+2.0}_{-1.7}$	CDF	[55]	lepton plus jets	34	9.2 ± 1.5
				40	22.6 ± 2.8
$8.2^{+4.4}_{-3.4}$	CDF	[56]	dileptons	9	2.4 ± 0.5
$10.1^{+4.5}_{-3.6}$	CDF	[57]	all jets , >0 tags	187	142 ± 12
			all jets , >1 tag	157	120 ± 18
$7.6^{+1.8}_{-1.5}$	CDF	[55]	CDF combined		
$4.7 - 5.8$	Theory	[58]	for m_t 173-175 GeV/c^2		

TABLE 9. Top Quark Mass Measurements.

m_t (GeV/c^2) (pb)	Source	Ref.	Method	Total Events	Background Events
$173.3 \pm 5.6 \pm 5.5$	DZero	[59]	lepton plus jets	76	53.2^{+11}_{-9}
					48.2^{+11}_{-9}
$168.4 \pm 12.3 \pm 3.6$	DZero	[60]	dileptons	6	
$172.1 \pm 5.2 \pm 4.9$	DZero	[59]	DZero combined		
$175.9 \pm 4.8 \pm 4.9$	CDF	[61]	lepton plus jets	76	31 ± 8
$161 \pm 17 \pm 10$	CDF	[62]	dileptons	9	2.4 ± 0.5
$186 \pm 10 \pm 12$	CDF	[63]	all jets , >0 tags	187	142 ± 12
			all jets, > 1 tag	157	120 ± 18
$173.8 \pm 3.5 \pm 3.9$	PDG	[64]	PDG Average		

Top Quark Production Cross Section

Table 8 gives the observed cross section results from both CDF and DZero. The events listed in the table come from approximately 100 pb^{-1} of data, meaning that about 500 $t\bar{t}$ events were produced in each experiment. Thus, CDF and DZero saw about 10 % of the top events produced, even after their final selection criteria were applied. That is quite efficient for such rare events. For those signatures with the most observed events, the backgrounds are the greatest. Nevertheless, the various data sets are consistent with each other, and consistently above the expected backgrounds.

Top Quark Mass Measurement

As suggested in the discussion of the cross section, kinematic fits to the events can leave the value of the t-quark mass free, only demanding that both the t and $\bar{t}$ have the same mass. Table 9 shows the results of the fits of essentially the same events as were used for the cross section measurements. Again, agreement of the various sets and between the two experiments gives confidence in the basic result.

Relation Between Mass and Cross Section and Other Tests

Given that the top quark mass is above the Wb threshold, the decay width should be about 1 GeV, corresponding to a lifetime of about 10^{-23} seconds. Thus, the t decays before top-hadrons or onia form. This is why the decay is totally dominated by the W b decay mode. The production cross section is calculated in NLO perturbative QCD. The perturbative calculation is expected to be very reliable. It does depend on the mass of the top quark, of course. Any inconsistency of the production rate and measured mass would cast doubt on the discovery. No discrepancy is observed, as seen in Table 8.

On the other hand, discrepancies might indicate exotic production channels, as could an unexpected distribution of the measured $t\bar{t}$ mass distribution and the distribution of the transverse momentum of the t. Angular distributions are sensitive to the presumed V-A coupling and the relative coupling of transverse and longitudinal W's to t. The fraction of decays to transversely and longitudinally polarized W's for 175 GeV/c^2 t is 30 %. A discrepancy would challenge the Higgs mechanism of spontaneous symmetry breaking. Finally, one can also imagine seeing clues to new physics via rare or forbidden decay rates. Finally, the top could be the source of observation of non-Standard Model particles. For example, if the Higgs particle were light enough, the top quark could decay emitting a Higgs particle. One could also be sensitive to decays to light enough SUSY particles.

THE NEXT HEAVY PARTICLES, THEIR OBSERVATION AND NATURE

In the search for heavier objects, heavy quarks will play a critical role as tags for the discovery of those heavier objects, and as a key to identifying what they are. We have seen how this was the case in the top discovery, where heavy quarks in jets separated top events from others among the highest p_t interactions.

Predictions for the Higgs Particle

The Higgs mechanism for electroweak symmetry breaking manifests itself in a particle whose coupling to another particle is proportional to the other particle's mass. Thus, Standard Model predictions of the Higgs mass can be made via virtual loop corrections for mass of the top quark. Note that the dependence of the W mass on the top mass is linear, while the dependence is logarithmic on the Higgs mass. Today, there is a lot of focus on this prediction, as the competition between Fermilab and CERN to discover the Higgs is very intense. The Higgs branching ratio to other particles depends, also, on the Higgs mass – due to threshold and phase space effects. So, identifying a signal at a given mass as a Higgs particle depends on measuring the relative branching ratios to as many of the heavy quarks, WW, WW^*, ZZ, and ZZ^* states as are kinematically allowed. The asterisks in decays to WW^* and ZZ^* refer to virtual, intermediate decay particles, W^* and Z^* whose decay can be to kinematically allowed final states. Many physicists expect

that direct observation of a Higgs particle will be the next breakthrough discovery. On the other hand, surprises can happen.

Only Three Generations of Quarks?

Are the three generations of quark pairs truly the complete story? The limits on additional light neutrinos from Z^o decay do not necessarily prove this, since there could be a very heavy neutrino for a fourth generation. There are some limits on this from virtual effects in rare decays of heavy quarks.

Characterizing the Squarks and Higgs of SUSY

There is not enough time in these lectures to give an overview of SUSY. The topic has been well covered in the lectures of Cupatitzio Ramírez and Carlos Wagner. Let me only note that the host of predicted SUSY particles will place a premium on the detailed characterization of any candidate observations, as well as filling out the mass-spectrum of particles discovered. Thus, the heavy squark decays to the corresponding quark, as well as SUSY Higgs couplings are critical to the understanding of what will have been seen.

CONCLUDING COMMENTS

I would like to recommend some reading for more detail than I could give here, in particular: a review article by Harry Lipkin [65] for the state of thinking before the November Revolution of 1974, Ed Thorndike's summary of bottom quark physics [66], and the PDG summary by Michelangelo Mangano and Thomas Trippe [67] on top quarks.

We have seen that heavy quarks have been both interesting in their own right, and useful tools for understanding other things – from light-meson resonances to the high-mass extensions of the current Standard Model. I want to note again the importance played by applying new technology matched to physics opportunities. The precision tracking made possible by microelectronic advances would have been less interesting except for the few mm lifetimes of the charm and bottom quarks in the laboratory. The fantastic increase in computing and storage efficiency made possible the treatment of large amounts of data as required by the low cross sections for heavy quark production. Finally, we should also be a little humble amid all the excitement of the anticipated discoveries of the next heavy objects. In my brief review, we have seen many of the results fly in the face of "common knowledge" and general expectations.

Let me close by reiterating the wealth of rather recent progress in understanding the quark nature of matter, and the enjoyment that has come from being part of this, both from the physics and from technical efforts. I also want to thank our hosts and organizers for a most stimulating and enjoyable workshop.

REFERENCES

1. M. Gell-Mann, "Symmetries of Baryons and Mesons," Phys. Rev. **125**, 1067 (1962).
2. J.D. Bjorken, "Partons," *Proc. of the Int. Conf. on Duality and Symmetry in Hadron Physics*, Tel Aviv, Israel, 1971, pp. 98-115.
3. M.Y. Han and Y. Nambu, "Three Triplet Model with Double SU(3) Symmetry," Phys. Rev. B **139**, 1006 (1965); Y. Nambu and M.Y. Han, "Three Triplets, Paraquarks, and Colored Quarks," Phys. Rev. D **10**, 674 (1974).
4. M. Gell-Mann, "A Schematic Model of Baryons and Mesons," Phys. Lett. **8**, 214 (1964).
5. G.F. Chew, "Bootstrap Theory of Quarks," Nucl. Phys. B **151**, 237 (1979).
6. V.E. Barnes *et al.*, "Observation of a Hyperon with Strangeness -3," Phys. Rev. Lett. **12**, 204 (1964).
7. J.J. Aubert *et al.*, Phys. Rev. Lett. **33**, 1404 (1974).
8. J.-E. Augustin *et al.* Phys. Rev. Lett. **33**, 1406 (1974).
9. Mark I Collaboration, G. Goldhaber *et al.*, Phys. Rev. Lett. **37**, 255 (1976); I. Peruzzi *et al.*, Phys. Rev. Lett. **37**, 569 (1976).
10. E288 Collaboration, S.W. Herb *et al.* Phys. Rev. Lett. **39**, 252 (1977); W.R. Innes *et al.*, Phys. Rev. Lett. **39**, 1240 (1977).
11. PLUTO Collaboration, C. Berger *et al.*, Phys. Lett. B **76**, 243 (1978); DASP-2 Collaboration, C.W. Darden *et al.*, Phys. Lett. B **76**, 246 (1978) and Phys. Lett. B **78** 364 (1978); DESY/Hamburg/Heidelburg/MPI-Munich Collaboration, J.K. Bienlein *et al.*, Phys. Lett. B **78**, 360 (1978).
12. M. Kobayashi and T. Maskawa, "Renormalizable Theory of Weak Interaction," Prog. Theor. Phys. **49**, 652 (1973).
13. L. Wolfenstein, "Parametrization of the Kobayashi-Maskawa Matrix," Phys. Rev. Lett. **51**, 1945 (1983).
14. S.L. Glashow, J. Iliopoulos, and L. Maiani, "Weak Interactions with Lepton-Hadron Symmetry." Phys. Rev. D **2**, 1285 (1970).
15. J.D. Bjorken and S.L. Glashow, "Elementary Particles and SU(4)," Phys. Lett. **11**, 255 (1964).
16. V.L. Fitch *et al.*, "Search for D^* Production in Pion Nucleon Interactions," Phys. Rev. D **33**, 1486 (1986).
17. J. Martin *et al.*, "Use of the ECL-CAMAC Trigger Processor System for Recoil Missing Mass Triggers at the Tagged Photon Spectrometer at Fermilab," in *Topical Conference on the Application of Microprocessors to High-Energy Physics Experiments*, Geneva, Switzerland, May 4-6, 1981, CERN, Microproc. 1981, pp 164ff.
18. J.A. Appel, "Triggering for Charm, Beauty, and Truth," in *The Search for Charm, Beauty, and Truth at High Energies*, November 15-22, 1981, Erice, Italy, G. Bellini and S.C.C. Ting, eds., Plenum Press, New York, USA (1984), pp 555-560.
19. T. Nash *et al.*, "High Performance Parallel Computers for Science: New Developments at the Fermilab Advanced Computer Program," *Workshop on Computational Atomic and Nuclear Physics at One Gigaflop*, Oak Ridge, Tenn., Apr 14-16, 1988, Brazil Exper. Symp. 1987, pp 151; J. Biel *et al.*, Proc. Int. Conf. Computing in High Energy Physics, Asilomar, Feb. 2-6, 1987, Computer Physics Communications **45**, 331 (1987); C. Stoughton and D.J. Summers, Computers in Physics **6**, 371 (1992); F. Rinaldo and S. Wolbers, Computers in Physics **7**, 184 (1993); S. Bracker *et al.*, IEEE Trans. on Nucl. Sci. **43**, 2457 (1996).

20. The earliest successful use of SMDs in high energy physics experiments was by the NA11 collaboration at CERN, who did so much to develop these devices. B. Hyams *et al.*, Nucl. Inst. and Meth. **205**, 99 (1983). J. Kemmer, Nucl. Inst. and Meth. **169**, 499 (1980).
21. K. Niu, E. Mikumo, and Y. Maeda, "A Possible Decay in Flight of a New Type Particle," Prog. Theor. Phys. **46**, 1644 (1971).
22. G. Burdman, "Potential for Discoveries in Charm Meson Physics," in *Workshop on Tau Charm Factory, Argonne, IL, Jun 21-23, 1995*, J. Repond *ed.*, Argonne National Laboratory, June 21–23, 1995, AIP Conference Proceedings No. 349, pp 409-424, FERMILAB-Conf-95-281, hep-ph/9508349.
23. Ted Liu, hep-ph/9508415.
24. H. Nelson, hep-ex/9908021 for compilation, and for new physics.
25. CLEO Collaboration, J. Bartelt *et al.*, Phys. Rev. D **52**, 4860, (1995).
26. CLEO Collaboration, R. Godang *et al.*, Phys. Rev. Lett. **84**, 5038 (2000).
27. FOCUS Collaboration, J.M. Link *et al.*, Submitted to Phys.Lett.B, hep-ex/0005037, FERMILAB-PUB-00-112-E.
28. E791 Collaboration, E.M. Aitala *et al.*, Phys. Lett. B **421**, 405 (1998).
29. E791 Collaboration, E.M. Aitala *et al.*, Phys. Lett. B **403**, 377 (1997).
30. E687 Collaboration, P.L. Frabetti *et al.*, Phys. Rev. D **50**, R2953 (1994).
31. F. Buccella *et al.*, Phys. Lett. B **302**, 319 (1993);
    A. Pugliese and P. Santorelli, "Two Body Decays of D Mesons and CP Violating Asymmetries in Charged D Meson Decays," *Proc. Third Workshop on the Tau/Charm Factory*, Marbella, Spain, 1–6, June 1993, Edition Frontieres (1994), p. 387.
32. Z. Xing, Phys. Lett. B **353**, 313 (1995).
33. E771 Collaboration, T. Alexopoulos *et al*, Phys. Rev. Lett. **77**, 2380 (1996).
34. WA92 Collaboration, M. Adamovich *et al.*, Phys. Lett. B **408**, 469 (1997).
35. J.L. Hewett, "Searching for New Physics with Charm," SLAC-PUB-95-6821, hep-ph/9505246, to appear in *Proc. LISHEP95 Workshop*, Rio de Janeiro, Brazil, Feb. 20–22, 1995.
36. E653 Collaboration, K. Kodama *et al.*, Phys. Lett. B **345**, 85 (1995).
37. CLEO Collaboration, A. Freyberger *et al.*, Phys. Rev. Lett. **76**, 3065 (1996), Erratum-ibid. **77**, 2147 (1996).
38. E791 Collaboration, E.M. Aitala *et al.*, Phys. Rev. Lett. **76**, 364 (1996).
39. E687 Collaboration, P.L. Frabetti *et al.*, Phys. Lett. B **398**, 239 (1997).
40. CLEO Collaboration, D.M. Asner *et al.*, Phys. Rev. D **58**, 2001 (1998).
41. E791 Collaboration, E.M. Aitala *et al.*, Phys. Lett. B **462**, 401 (1999).
42. G. Burdman, "Charm Mixing and CP Violation in the Standard Model," in **The Future of High-Sensitivity Charm Experiments**, *Proc. CHARM2000 Workshop*, Fermilab, June 7–9, 1994, D. Kaplan and S. Kwan *eds.*, FERMILAB-Conf-94/190, p. 75, hep-ph/9407378.
43. E791 Collaboration, E.M. Aitala *et al.*, Phys. Rev. Lett. **77**, 2384 (1996).
44. Harry W.K. Cheung, "Review of Charm Lifetimes," in 8^{th} *International Symposium on Heavy Flavor Physics (Heavy Flavors 8)*, Southampton, England, 25-29 Jul 1999, hep-ex/9912021.
45. I. Bigi, M. Shifman, N.G. Uraltsev, and A. Vainshtein, "Nonperturbative Corrections to Inclusive Beauty and Charm Decays: QCD versus Phenomenological Models," Phys. Lett. B **293**, 430 (1992); Erratum-ibid. **297**, 477 (1993); I. Bigi and N.G.

Uraltsev, Z. fur Phys. C **62**, 623 (1994).
46. E791 Collaboration, E.M. Aitala *et al.*, Accepted for publication in Phys. Rev. Lett. hep-ex/0007027 and hep-ex/0007028.
47. A. Garren *et al.*, "An Asymmetric B Meson Factory at PEP," *Proc. Part. Accel. Conf.*, Chicago, Ill., Mar 20-23, 1989. IEEE Part. Accel. Conf. 1989, pp 1847-1849.
48. J.A. Appel *et al.*, "In Celebration of the Fixed Target Program with the Tevatron," http://conferences.fnal.gov/tevft/book/; hep-ex/0008076 for short version.
49. UA1 Collaboration, C. Albajar *et al.*, Phys. Lett. B **186**, 247 (1987).
50. CDF Collaboration, F. Abe *et al.*, Phys. Rev. Lett. **75**, 1451 (1995); **71**, 2537 (1993); **71**, 2396 (1993); **71**, 500 (1993).
51. D0 Collaboration, B. Abbott *et al.*, hep-ex/0008021; Phys. Rev. Lett. **84**, 5478 (2000); Phys. Lett. B **487**, 264 (2000).
52. CLEO Collaboration, R.A. Briere *et al.*, hep-ex/000428.
53. CDF Collaboration, F. Abe *et al.*, Phys. Rev. D **60**, 092005 (1999).
54. DZero Collaboration, S. Abachi *et al.*, Phys. Rev. Lett. **79**, 1203 (1997).
55. CDF Collaboration, F. Abe *et al.*, Phys. Rev. Lett. **80**, 2773 (1998).
56. CDF Collaboration, F. Abe *et al.*, Phys. Rev. Lett. **80**, 2779 (1998).
57. CDF Collaboration, F. Abe *et al.*, Phys. Rev. Lett. **79**, 1992 (1997).
58. P. Nason, S. Dawson, and R.K. Ellis, Nucl. Phys. B **303**, 607 (1988); W. Beenakker, H. Juijf, W.L. van Neerven, and J. Smith, Phys. Rev. D **40**, 54 (1989); E. Berger and H. Contopanagos, Phys. Lett. B **361**, 115 (1995); E. Laenen, J. Smith, and W. van Neerven, Phys. Lett. B **321**, 254 (1994); S. Catani, M. Mangano, P. Nason, and L. Trentadue, Phys. Lett. B **378**, 329 (1996).
59. DZero Collaboration, S. Abachi *et al.*, Phys. Rev. Lett. **79**, 1197 (1997).
60. DZero Collaboration, B. Abbott *et al.*, Phys. Rev. Lett. **80**, 2063 (1998).
61. CDF Collaboration, F. Abe *et al*, Phys. Rev. Lett. **80**, 2779 (1998).
62. CDF Collaboration, F. Abe *et al*, Phys. Rev. Lett. **79**, 1992 (1997).
63. CDF Collaboration, F. Abe *et al*, Phys. Rev. Lett. **80**, 2767 (1998).
64. Particle Data Group's "Review of Particle Properties," Eur. Phys. J. C **3**, 345 (1998).
65. H.J. Lipkin, "Quarks for Pedestrians," Phys. Rept. **8**, 173 (1973).
66. E.H. Thorndike, "Bottom Quark Physics: Past, Present, Future" in "Symposium on Probing Luminous and Dark Matter, honoring Adrian Melissinos," Rochester, New York, USA, October, 1999, hep-ex/0003027.
67. M. Mangano and T. Trippe, "The Top Quark" in Particle Data Group's "Review of Particle Properties," Eur. Phys. J. C **3**, 343 (1998).